Journal of Instrumentation

SISSA

OPEN ACCESS

Triple-GEM discharge probability studies at CHARM: simulations and experimental results

To cite this article: M. Abbas *et al* 2020 *JINST* **15** P10013

Published by IOP Publishing for Sissa Medialab

Received: *June 24, 2020*
Accepted: *August 24, 2020*
Published: *October 15, 2020*

Triple-GEM discharge probability studies at CHARM: simulations and experimental results

M. Abbas,[n] M. Abbrescia,[t] H. Abdalla,[h,j] A. Abdelalim,[h,k] S. AbuZeid,[h,i] A. Agapitos,[d] A. Ahmad,[ad] A. Ahmed,[q] W. Ahmed,[ad] C. Aimè,[y] I. Asghar,[ad] P. Aspell,[ah] C. Avila,[f] J. Babbar,[p] Y. Ban,[d] R. Band,[aj] S. Bansal,[p] L. Benussi,[v] V. Bhatnagar,[p] M. Bianco,[ah] S. Bianco,[v] K. Black,[am] L. Borgonovi,[u] O. Bouhali,[ae] A. Braghieri,[y] S. Braibant,[u] S. Butalla,[an] S. Calzaferri,[y] M. Caponero,[v] F. Cassese,[x] N. Cavallo,[x] S. Chauhan,[p] S. Colafranceschi,[an] A. Colaleo,[t] A. Conde Garcia,[ah] M. Dalchenko,[ai] A. De Iorio,[x] G. De Lentdecker,[a] D. Dell Olio,[t] G. De Robertis,[t] W. Dharmaratna,[ag] S. Dildick,[ai] B. Dorney,[a] R. Erbacher,[aj] F. Fabozzi,[x] F. Fallavollita,[ah] A. Ferraro,[y] D. Fiorina,[y] E. Fontanesi,[u] M. Franco,[t] C. Galloni,[am] P. Giacomelli,[u] S. Gigli,[y] J. Gilmore,[ai] M. Gola,[q] M. Gruchala,[ah] A. Gutierrez,[ak] R. Hadjiiska,[c] T. Hakkarainen,[l] J. Hauser,[al] K. Hoepfner,[m] M. Hohlmann,[an] H. Hoorani,[ad] T. Huang,[ai] P. Iaydjiev,[c] A. Irshad,[a] A. Iorio,[x] J. Jaramillo,[g] D. Jeong,[ab] V. Jha,[s] A. Juodagalvis,[ac] E. Juska,[ai] B. Kailasapathy,[af] T. Kamon,[ai] P. Karchin,[ak] A. Kaur,[p] H. Kaur,[p] H. Keller,[m] H. Kim,[ai] J. Kim,[aa] A. Kumar,[q] S. Kumar,[p] H. Kumawat,[s] N. Lacalamita,[t] J.S.H. Lee,[ab] A. Levin,[d] Q. Li,[d] F. Licciulli,[t] L. Lista,[x] K. Liyanage,[ag] F. Loddo,[t] M. Lohan,[p] M. Luhach,[p] M. Maggi,[t] N. Majumdar,[r] K. Malagalage,[af] S. Malhorta,[ae] S. Martiradonna,[t] N. Mccoll,[al] C. McLean,[aj] J. Merlin,[t] D. Mishra,[s] G. Mocellin,[m] L. Moureaux,[a] A. Muhammad,[ad] S. Muhammad,[ad] S. Mukhopadhyay,[r] M. Naimuddin,[q] P. Netrakanti,[s] S. Nuzzo,[t] R. Oliveira,[ah] L. Pant,[s] P. Paolucci,[x] I.C. Park,[ab] L. Passamonti,[v] G. Passeggio,[x] A. Peck,[al] N. Perera,[ag] L. Petre,[a] H. Petrow,[l] D. Piccolo,[v] D. Pierluigi,[v] G. Raffone,[v] M. Rahmani,[an] F. Ramirez,[g] A. Ranieri,[t] G. Rashevski,[c] M. Ressegotti,[y,1] C. Riccardi,[y] M. Rodozov,[c] E. Romano,[y] C. Roskas,[b] B. Rossi,[x] P. Rout,[r] J.D. Ruiz,[g] A. Russo,[v] A. Safonov,[ai] D. Saltzberg,[al] G. Saviano,[v] A. Shah,[q] A. Sharma,[ah] R. Sharma,[q] M. Shopova,[c] F. Simone,[t] J. Singh,[p] E. Soldani,[t] U. Sonnadara,[af] E. Starling,[a] B. Stone,[al] J. Sturdy,[ak] G. Sultanov,[c] Z. Szillasi,[o] D. Teague,[am] D. Teyssier,[o] T. Tuuva,[l] M. Tytgat,[b] I. Vai,[w,2] N. Vanegas,[g] R. Venditti,[t] P. Verwilligen,[t] W. Vetens,[am] A. Virdi,[p] P. Vitulo,[y] A. Wajid,[ad] D. Wang,[d] K. Wang,[d] I. Watson,[ab] N. Wickramage,[ag] D.D.C. Wickramarathna,[af] Y. Yang,[a] U. Yang,[aa] J. Yongho,[z] I. Yoon,[aa] Z. You,[e] I. Yu[z] and S. Zaleski[m] on behalf of the CMS Muon Group

[1]Now at INFN Sezione di Genova, Genova, Italy.
[2]Corresponding author.

https://doi.org/10.1088/1748-0221/15/10/P10013

2020 JINST 15 P10013

[a] Université Libre de Bruxelles, Bruxelles, Belgium
[b] Ghent University, Ghent, Belgium
[c] Institute for Nuclear Research and Nuclear Energy, Sofia, Bulgaria
[d] Peking University, Beijing, China
[e] Sun Yat-Sen University, Guangzhou, China
[f] University de Los Andes, Bogota, Colombia
[g] Universidad de Antioquia, Medellin, Colombia
[h] Academy of Scientific Research and Technology — ENHEP, Cairo, Egypt
[i] Ain Shams University, Cairo, Egypt
[j] Cairo University, Cairo, Egypt
[k] Helwan University, Helwan, Egypt[3]
[l] Lappeenranta University of Technology, Lappeenranta, Finland
[m] RWTH Aachen University, III. Physikalisches Institut A, Aachen, Germany
[n] Karlsruhe Institute of Technology, Karlsruhe, Germany
[o] Institute for Nuclear Research ATOMKI, Debrecen, Hungary
[p] Panjab University, Chandigarh, India
[q] Delhi University, Delhi, India
[r] Saha Institute of Nuclear Physics, Kolkata, India
[s] Bhabha Atomic Research Centre, Mumbai, India
[t] Politecnico di Bari, Università di Bari and INFN Sezione di Bari, Bari, Italy
[u] Università di Bologna and INFN Sezione di Bologna, Bologna, Italy
[v] Laboratori Nazionali di Frascati INFN, Frascati, Italy
[x] Università di Napoli and INFN Sezione di Napoli, Napoli, Italy
[y] Università di Pavia and INFN Sezione di Pavia, Pavia, Italy
[w] Università di Bergamo and INFN Sezione di Pavia, Pavia, Italy
[z] Korea University, Seoul, Korea
[aa] Seoul National University, Seoul, Korea
[ab] University of Seoul, Seoul, Korea
[ac] Vilnius University, Vilnius, Lithuania
[ad] National Center for Physics, Islamabad, Pakistan
[ae] Texas A&M University at Qatar, Doha, Qatar
[af] University of Colombo, Colombo, Sri Lanka
[ag] University of Ruhuna, Matara, Sri Lanka
[ah] CERN, Geneva, Switzerland
[ai] Texas A&M University, College Station, U.S.A.
[aj] University of California, Davis, Davis, U.S.A.
[ak] Wayne State University, Detroit, U.S.A.
[al] University of California, Los Angeles, U.S.A.
[am] University of Wisconsin, Madison, U.S.A.
[an] Florida Institute of Technology, Melbourne, U.S.A.

E-mail: ilaria.vai@unibg.it

[3] Also at Zewail City of Science and Technology, Cairo, Egypt.

2020 JINST 15 P10013

Abstract: The CMS muon system in the region with $2.03 < |\eta| < 2.82$ is characterized by a very harsh radiation environment which can generate hit rates up to 144 kHz/cm^2 and an integrated charge of 8 C/cm^2 over ten years of operation. In order to increase the detector performance and acceptance for physics events including muons, a new muon station (ME0) has been proposed for installation in that region. The technology proposed is Triple — Gas Electron Multiplier (Triple-GEM), which has already been qualified for the operation in the CMS muon system. However, an additional set of studies focused on the discharge probability is necessary for the ME0 station, because of the large radiation environment mentioned above. A test was carried out in 2017 at the Cern High energy AcceleRator Mixed (CHARM) facility, with the aim of giving an estimation of the discharge probability of Triple-GEM detectors in a very intense radiation field environment, similar to the one of the CMS muon system. A dedicated standalone Geant4 simulation was performed simultaneously, to evaluate the behavior expected in the detector exposed to the CHARM field. The geometry of the detector has been carefully reproduced, as well as the background field present in the facility. This paper presents the results obtained from the Geant4 simulation, in terms of sensitivity of the detector to the CHARM environment, together with the analysis of the energy deposited in the gaps and of the processes developed inside the detector. The discharge probability test performed at CHARM will be presented, with a complete discussion of the results obtained, which turn out to be consistent with measurements performed by other groups.

Keywords: Detector modelling and simulations I (interaction of radiation with matter, interaction of photons with matter, interaction of hadrons with matter, etc); Avalanche-induced secondary effects; Micropattern gaseous detectors (MSGC, GEM, THGEM, RETHGEM, MHSP, MICROPIC, MICROMEGAS, InGrid, etc)

2020 JINST 15 P10013

Contents

2020 JINST 15 P10013

1 Motivation

To meet the challenges that the High-Luminosity (HL-LHC) upgrade of the LHC will bring, the CMS collaboration will improve the muon system. Among the new detector stations that are proposed for the installation, the ME0 station will be installed in the region $2.0 < |\eta| < 2.82$ (figure 1) during Long Shutdown 3 (LS3). The main motivation for the insertion of the ME0 station is to increase the CMS acceptance for physics with muons. In particular, this short section of muon detector (~ 40 cm) could increase the muon acceptance by $\sim 10\%$ [1].

The technology to be installed in the ME0 station should be able to discriminate muons from neutrons and γ background, and to find muon stubs among background hits. The expected background fluxes in the ME0 region can reach up to $\sim 5 \times 10^6\,\mathrm{cm^{-2}\,s^{-1}}$, for an expected overall particle rate of the order of 144 kHz/cm^2 and an integrated charge up to ~ 8 C/cm^2 in ten years of operation of HL-LHC in the sectors closest to the beam line, and ~ 1.2 C/cm^2 on average on the entire single detector surface.

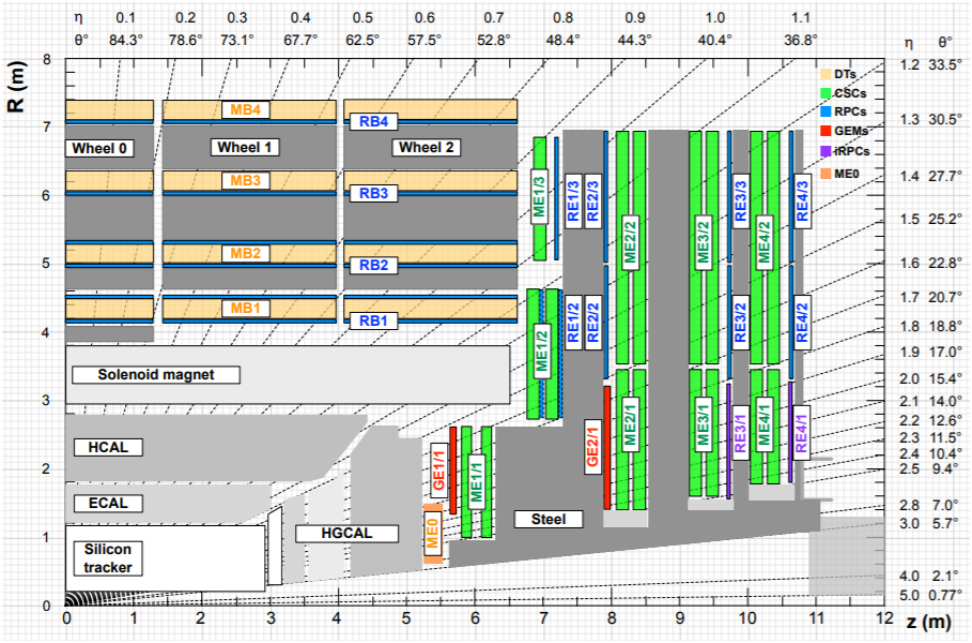

Figure 1. Overview of the CMS muon system upgrade [2]. The region marked in orange will host the entire ME0 structure, as shown in figure 2.

The technology proposed for the ME0 installation is Triple-GEM detectors [3], similar to those that will be first used for the GE1/1 station after LS2. Each ME0 stack will be composed of six chambers, arranged as in figure 2. The grey part is the structure with the six layers of GEM detectors, while the green box is the electronics volume [2].

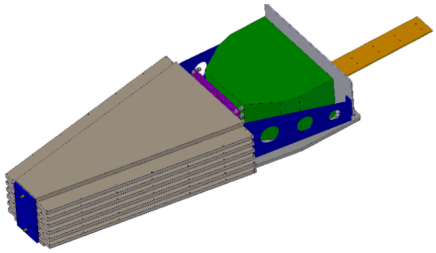

Figure 2. Stack of six Triple-GEM detectors for the ME0 station [2].

The qualification of operation of Triple-GEM detectors in a hostile radiation environment was already partially performed during the GE1/1 (the first new GEM station) R&D phase, when an integrated charge of 55 mC/cm^2 was reached without degradation of performance [4]. A continuation of this test was performed at the Gamma Irradiation Facility++ (GIF++) [5] at CERN and in the CMS-GEM QA/QC laboratory at CERN with X-rays, where integrated charges of 218 mC/cm^2 (3% of the expected charge in ten years of HL-LHC in the hottest sector of ME0) and 1.5 C/cm^2 were reached respectively [6]. This latest value in particular represents about 19% of the expected charge in ten years of LHC operation in the hottest sector and a full qualification (with safety factor 1.25) if considering the average charge accumulated over the detector surface. However, a test dedicated

2020 JINST 15 P10013

to the measurement of discharge probability in an environment similar to the one of the CMS muon system was also necessary to fully qualify the operation of the detectors. Indeed, discharges are the main general problem for Micropattern Gaseous Detectors (MPGD), including GEM, since they can prevent the detector from working properly or even destroy it completely.

2 Triple-GEM detector prototype

The detector irradiated in the test was a Triple-GEM detector prototype, consisting of 10 cm × 10 cm GEM-foil developed and produced with a single-mask photolithography technique, with gap sizes of 3/1/2/1 mm, as shown in figure 3. The read-out board consists of 81 pads of $1 \times 1\,\mathrm{cm}^2$ size. All the readout pads were routed to a 128-pin Panasonic connector. To power a Triple-GEM, a total of seven different high-voltage potentials were applied to its layers, using the CAEN A1515TG multi-channel HV power supply [7], specifically designed for Triple-GEM detectors. One A1515TG module provides fourteen floating HV channels that are grouped in two complex channels. Within a complex channel, the seven channels can be configured individually. The floating design assures that the failure of one channel shall not result in an increase of the potential on the neighboring layer. The characteristics of this board are discussed in detail in ref. [7]. The typical configuration of potentials in the Triple-GEM detector is shown in figure 3. A 10 MΩ protection resistor was mounted on the upper electrode of each GEM-foils, and a HV low-pass filter composed of 100 kΩ resistors and 2.2 nF capacitors was employed on the lower electrode of each GEM-foils in order to diminish the high frequency noise from the HV power supply. Moreover, different GEM filter configurations can mitigate the discharge propagation and hence play an important role. Consequently, the discharge probability may be different according to the different detector layouts.

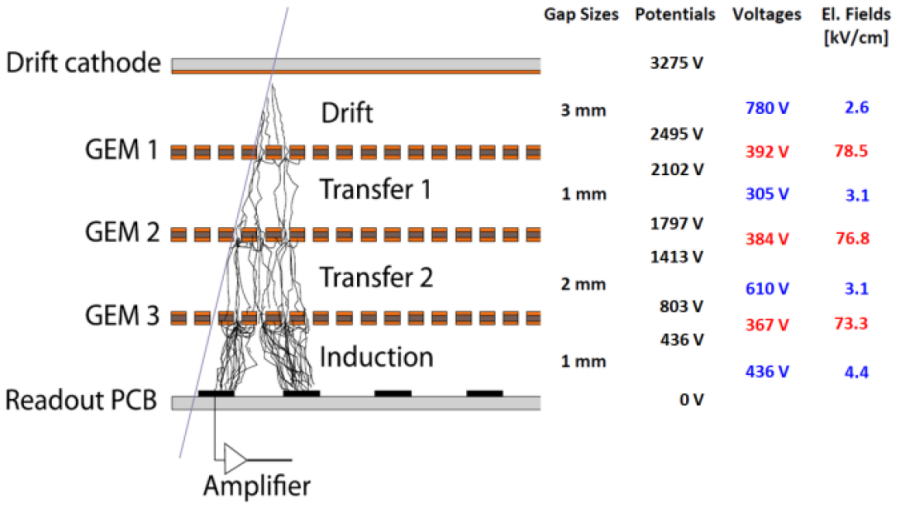

Figure 3. Schema of a Triple-GEM detector together with the typical values of potential, voltage and electric field for the operation.

2020 JINST 15 P10013

3 Discharge in GEM-based detectors

In a GEM-based detector, the discharge starts with a sudden, radiation-induced breakdown of the gas rigidity in one GEM, normally the last one in a cascade of multipliers. Studies performed in the past [8] show that the probability of this initial discharge could depend on the primary ionization density, on the overall gain of the structure and on the composition of the radiation environment, but not directly on the external fields. In particular, the discharge voltage decreases when moving from a single GEM structure to a multiple GEM structure, because the avalanche size for a multiple-layer device is bigger than for a single foil device. The maximum gain achievable before discharge is increased by almost an order of magnitude at each addition of a multiplier layer, reaching about 10^5 for a triple GEM structure [8]. Many discharge probability measurements have been performed in the past years, with GEM detectors of different geometries. The results obtained often vary by orders of magnitude, emphasising that this phenomenon is strongly dependent on the geometry of the detector, the gas mixture used, and the operational conditions [9–11].

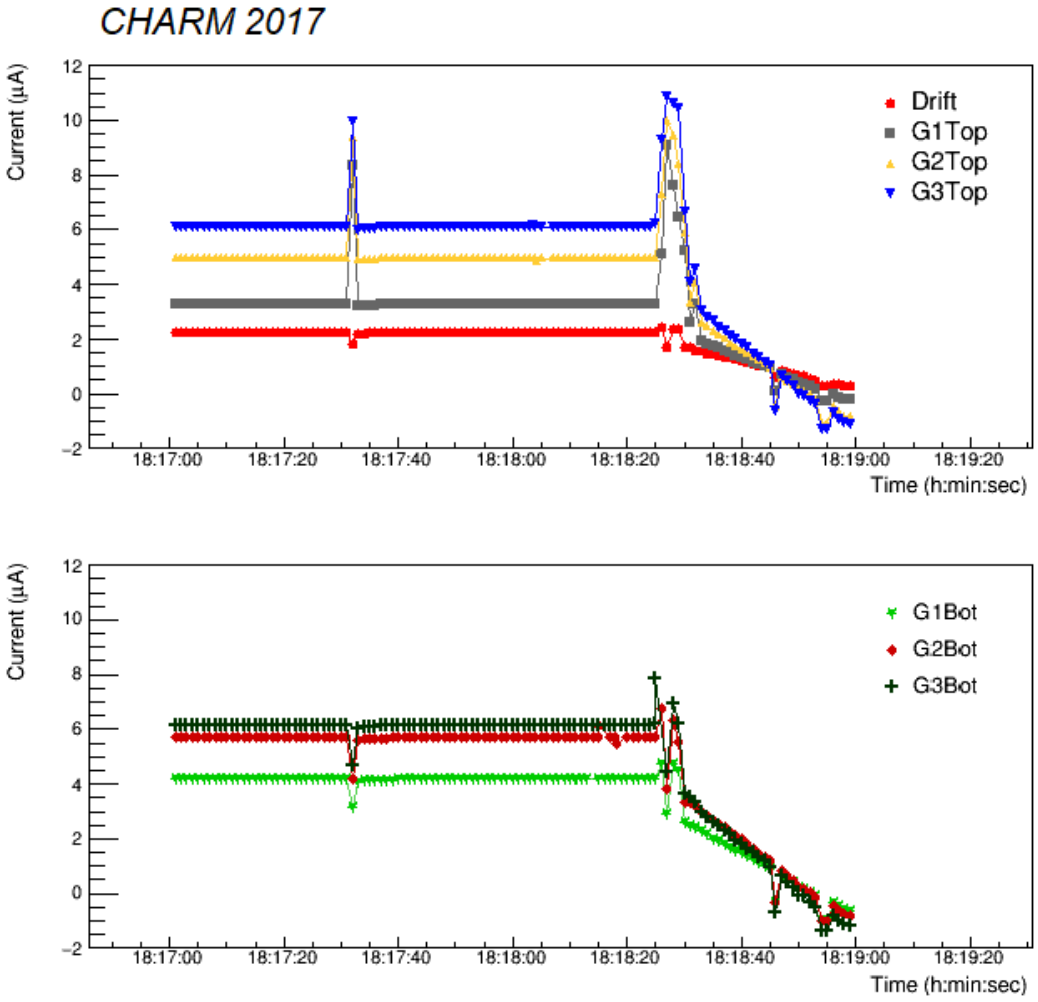

Figure 4. Discharge induced on a Triple-GEM detector during the tests performed in laboratory before the CHARM irradiation.

A discharge pattern observed during the test is shown in figure 4. This discharge was induced on a Triple-GEM detector during the preliminary tests performed in the CMS-GEM QA/QC laboratory at CERN before the irradiation with a 1 MBq ^{109}Cd + 1 MBq ^{55}Fe + 25 MBq ^{109}Cd source. The gain of the Triple-GEM detector was 3×10^5. The discharge presented a first small peak, which is positive on the top channels (top plot) and negative on the bottom channels (bottom plot), too fast to trigger a channel trip, followed by a larger spike about 60 seconds later that triggered a channel trip. The current limit on each channel of the high voltage module was set 1 µA above the average current measured with the source on the detector, with a trip time of 1 sec. In addition, the high voltage module was used in *GEM mode* (see [7] for details), in such a way that a trip on a single channel would induce the shutdown of the entire detector, for safety reasons. This explains why all the channels were turned off after the second spike, even if only few of them actually exceeded the current limit.

4 The CHARM facility

The facility selected for the discharge probability test was the Cern High energy AcceleRator Mixed (CHARM) field/facility [12], built at CERN in the Proton Synchrotron (PS) east area (see figure 5 left).

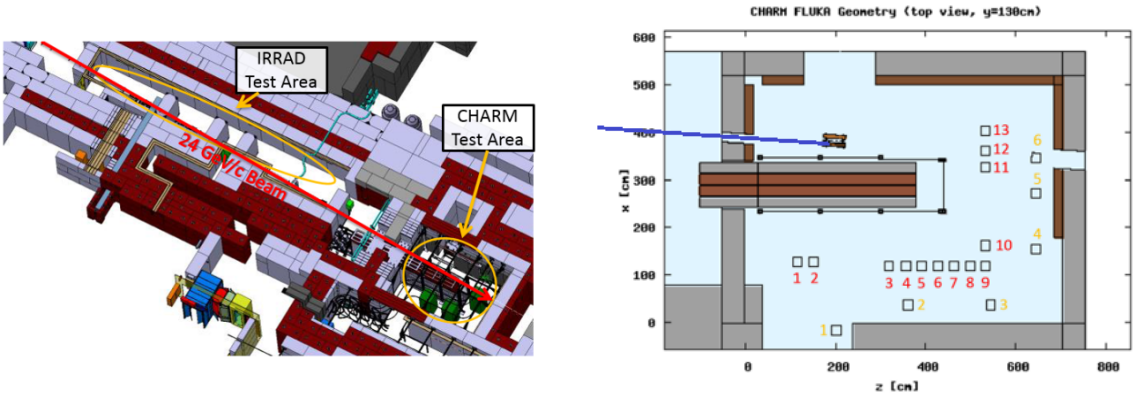

Figure 5. Left: overview of the CHARM facility along the PS beam line [12]. Right: screen-shot of the test positions as reproduced in the CHARM FLUKA geometry, cut at beam-height. The different irradiation position are shown in red [12]. The blue line represents the beam line.

The CHARM radiation field is produced by the interaction of the 24 GeV/c PS beam with a cylindrical copper or aluminium target. The High Energy Hadrons (HEH) radiation field produced is mainly composed of neutrons, protons, pions, kaons and muons. In addition, a high intensity flux of gammas is also present. The intensity of the radiation field is different in the various irradiation positions: for our test the position R3, indicated as a red 3 in figure 5 right, was used. The CHARM facility is also equipped with an array of shielding blocks of concrete (grey rectangles) and iron (brown rectangles) as shown in figure 5 right [12]. During our test, the full shielding was used, the irradiation configuration is called *R3 with CuCIIC* (Cu target and Concrete + Iron + Iron + Concrete shielding), where Cu represents the copper target for the beam.

Figure 6 shows the normalized fluence in the irradiation position: the wider spectrum is from neutrons, going from 10^{-9} MeV to 10^3 MeV. The contribution of the other particle spectra is relevant only for energies higher than 100 keV.

2020 JINST 15 P10013

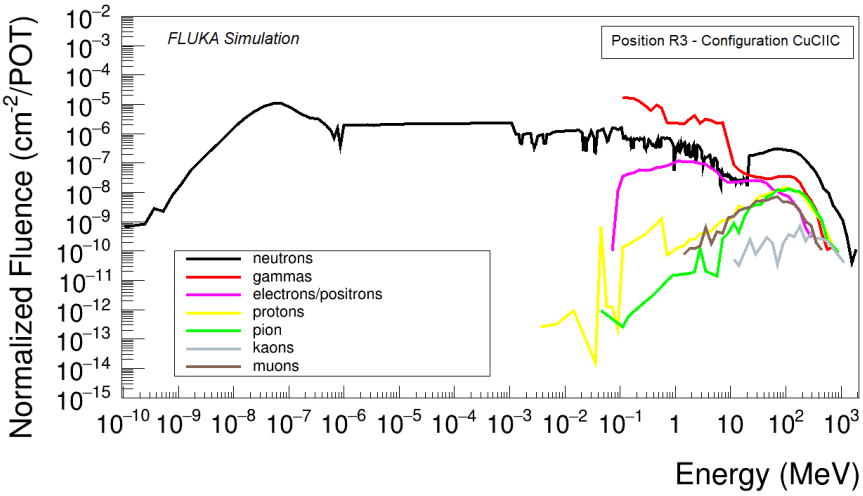

Figure 6. Spectrum of the different particle species present in the irradiation position, expressed in cm^{-2}/POT, where POT means *Proton on Target*. The data come from a FLUKA simulation performed by the CHARM personnel [13].

5 Geant4 simulation

To understand the behavior of a Triple-GEM detector immersed in the CHARM field, a dedicated Geant4 [14] simulation was performed. The aim of this simulation is to estimate the sensitivity of the Triple-GEM detector to the CHARM particles, i.e. the probability for a background particle to generate a minimum detectable signal in the detector. For this estimate, the geometry of the detector has been then carefully reproduced including the following elements:

- Standard Triple-GEM detector, $10 \times 10\,cm^2$, with a gap configuration 3/1/2/1 mm
- Kapton window, 50 µm-thick, plus FR4 layer, 1.2 mm-thick, on top, as done during the irradiation[1]
- Gas gaps filled with Ar/CO_2 (70/30).

The detector was then fixed to an aluminum support, included as well in the latest version of the simulation.

In parallel, the spectrum of every component of the CHARM radiation field in the irradiation position was obtained from a sampling of the complete spectrum shown in figure 6.

5.1 Sensitivity results

The sensitivity (S) of the Triple-GEM detector to each particle species composing the CHARM radiation field is then calculated as

$$S = \frac{N}{M} \tag{5.1}$$

where N is the number of signals in the detector, while M is the number of incident particles. We assume that the detector gives a signal if at least one charged particle reaches one of the first two gas

[1]The FR4 layer on top of the detector was added to reproduce as much as possible the geometry of a CMS Triple-GEM detector, which is closed by a 3.2 mm FR4-based drift board.

2020 JINST 15 P10013

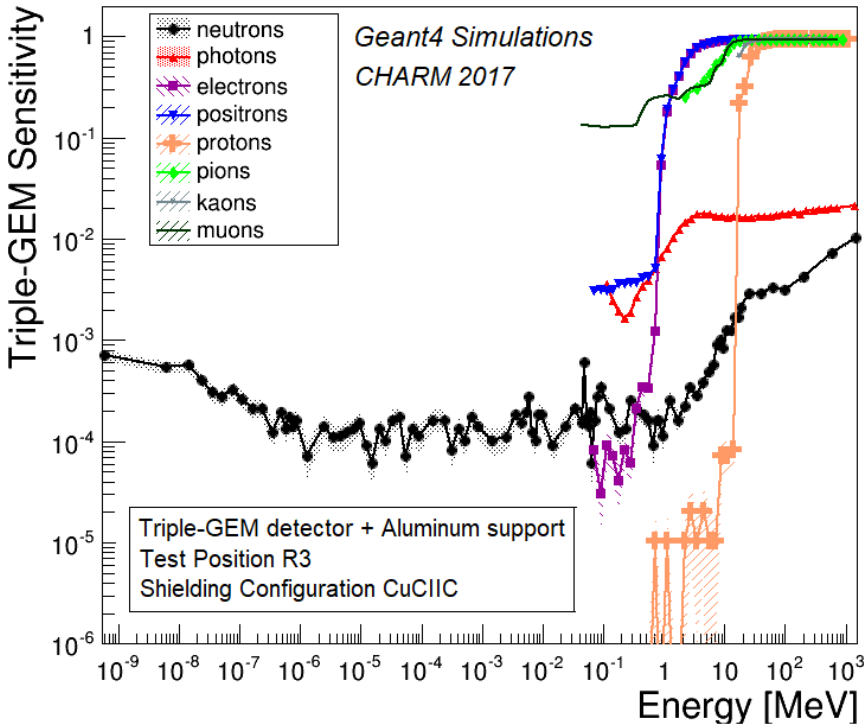

Figure 7. Sensitivity of the Triple-GEM detector exposed to the CHARM flux as a function of the energy of the incident particle for the different particle species present.

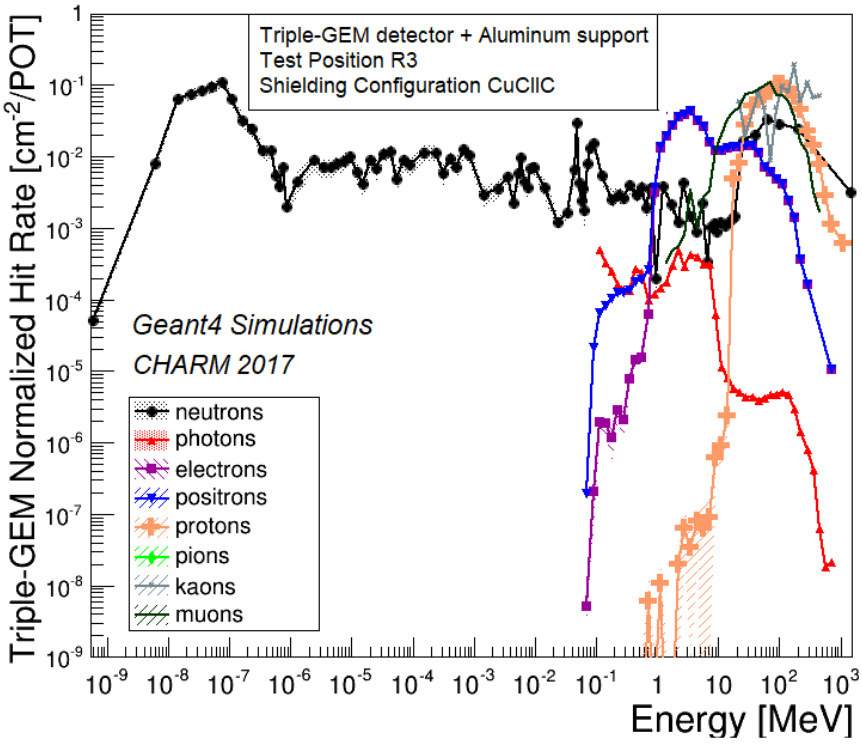

Figure 8. Hit rate of the Triple-GEM detector exposed to the CHARM flux as a function of the energy of the incident particle for the different particle species present.

2020 JINST 15 P10013

gaps of the Triple-GEM detectors. Of course, this assumption leads to the estimation of an upper limit for the sensitivity. Figure 7 shows the sensitivity as a function of the energy of the incident particle for the different particle species present in CHARM.

Convolving the sensitivity with the particle spectra, the hit rate is obtained (figure 8). It is useful to understand which particle gives the highest contribution in each energy range. Up to 1 MeV, neutrons are dominant, whereas at higher energy ranges their contribution drops in favour of the different species of charged particles.

5.2 Energy deposited results

An additional analysis was performed on the energy deposited by the particle into the different gas gaps. Each gas gap has been considered independently and the average total energy deposited has been analyzed. Figure 9 shows the result of this study for the drift gap as a function of the energy of the incident particle for the different particle species present.

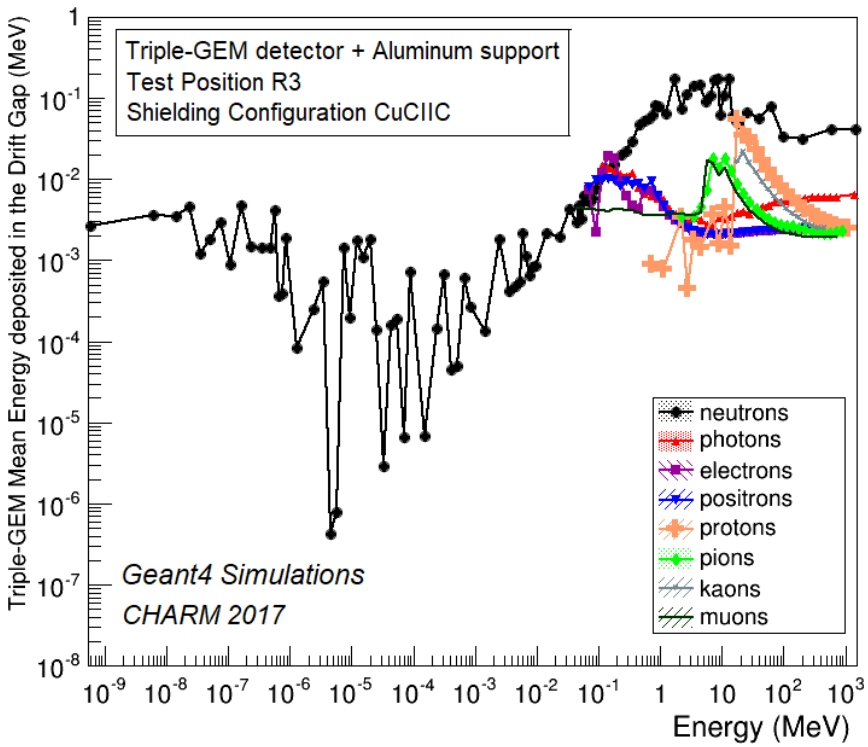

Figure 9. Average total energy deposited into the drift gap by particles hitting the detector as a function of the energy of the incident particle.

Overall, this analysis demonstrated that the total energy deposited can reach up to ~100 keV for photons and ~1 MeV for neutrons, the two predominant components of the CMS background.

5.3 Analysis of the physics processes

Interesting information on the functioning of the Triple-GEM detector is obtained from the analysis of the physics processes that develop in the detector when hit by a particle. This study has been performed for neutrons and photons in the CHARM energy range and the results are shown in figure 10 and 11 respectively.

2020 JINST 15 P10013

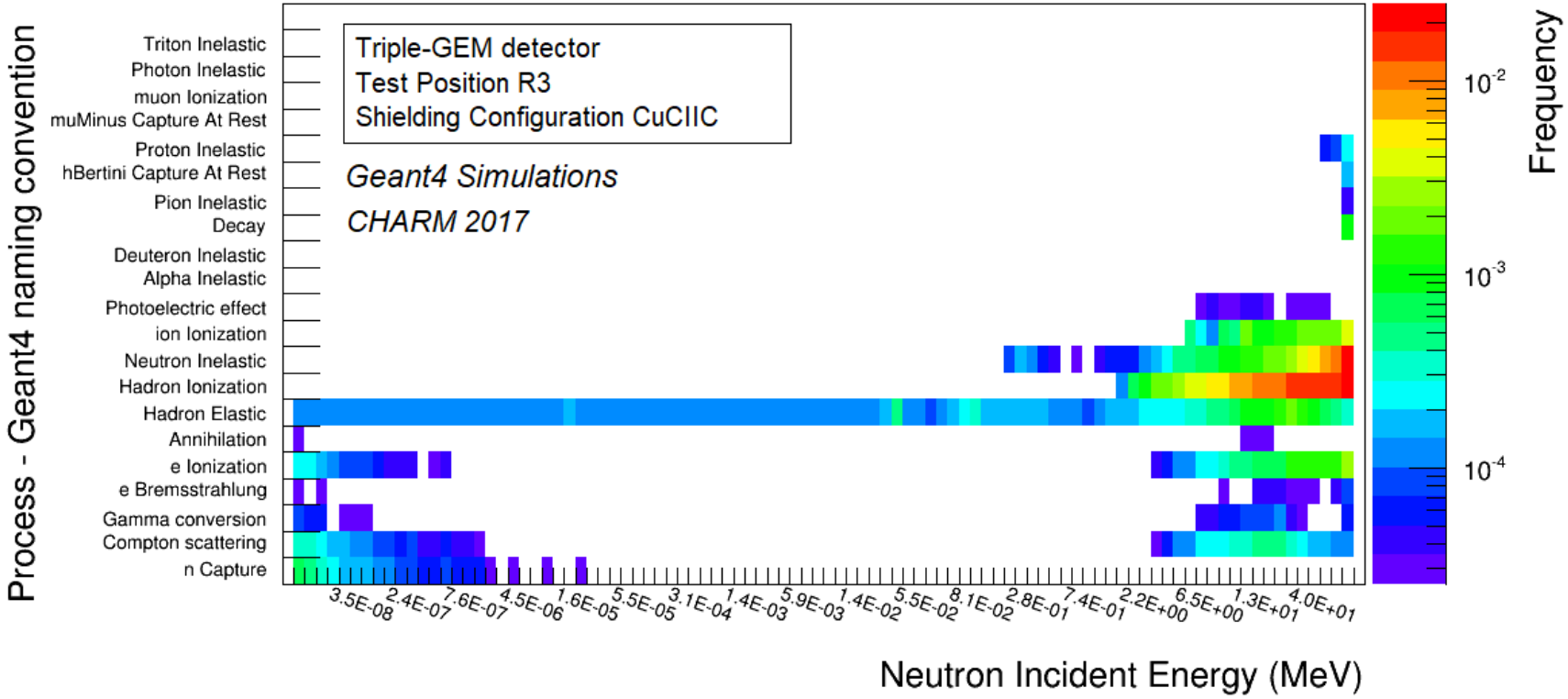

Figure 10. Processes undergone by neutrons when entering the Triple-GEM detector.

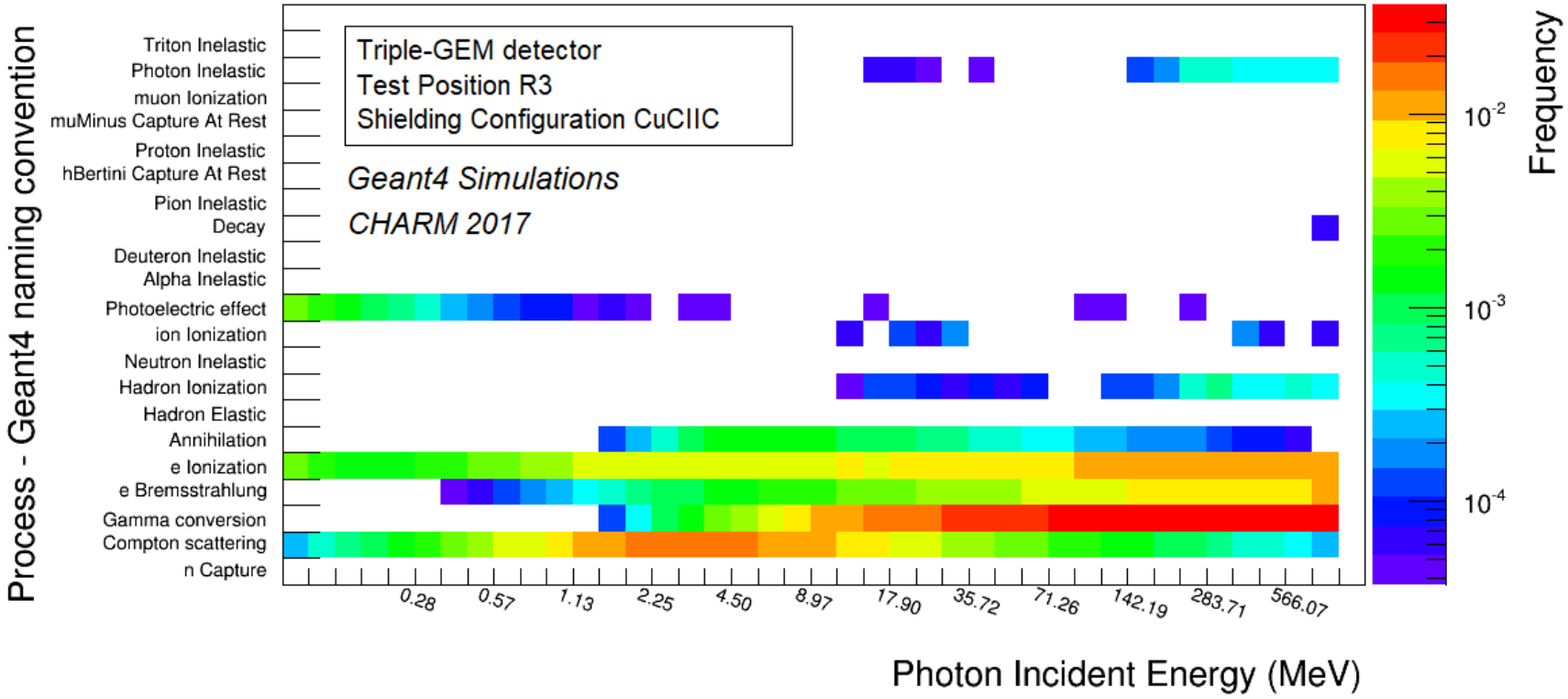

Figure 11. Processes undergone by photons when entering the Triple-GEM detector.

For the neutron processes, three regions can be identified: at low energies (E < 10 eV) neutron capture processes are dominant; at intermediate energies (up to 1 MeV) the elastic scattering is dominant; at high energies (E > 1 MeV) the inelastic reactions are dominant.

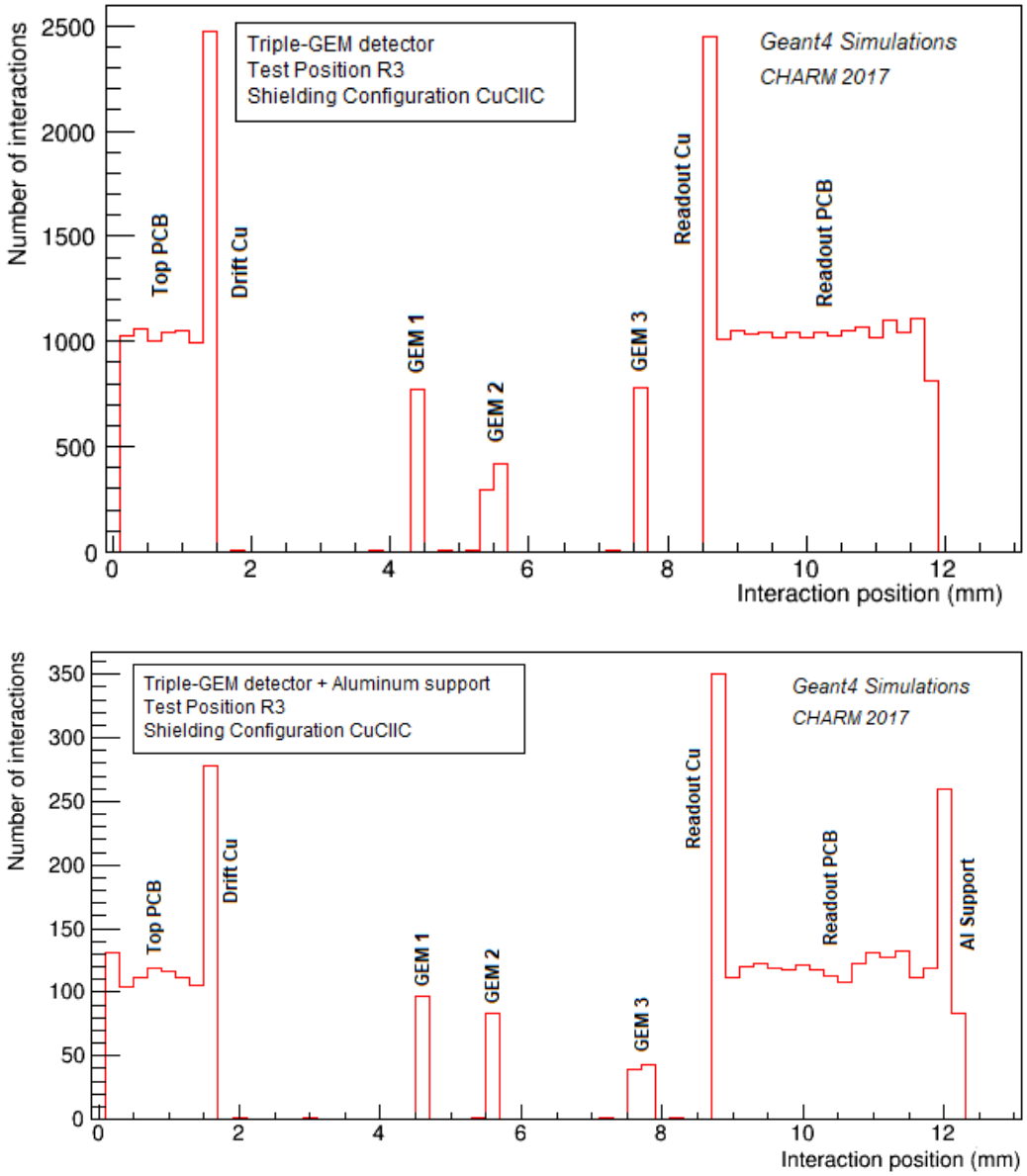

Figure 12. Position of the interactions undergone by photons in the Triple-GEM detector. Top: without the aluminum support. Bottom: with the aluminum support included in the simulation.

For photon processes three regions are also identified: at low energies (E < 0.3 MeV) the photoelectric effect is dominant; at intermediate energies (up to 18 MeV) the Compton scattering is dominant; at higher energies (E > 18 MeV) the pair production is dominant.

The regions with higher interaction number are the readout board and the shielding FR4 placed on top of the detector for both photons (figure 12) and neutrons (figure 13). In particular, the contribution coming from the interaction of photons with the Cu layer of the readout and of the

2020 JINST 15 P10013

drift board (figure 12) is obvious. Some interactions also occur in the GEM foils themselves. On the other hand, in the gas gaps the interaction probability for photons is much lower. In the plot with the aluminum support (figure 12 bottom), a peak caused by the support itself can be identified at z = 12.5 mm.

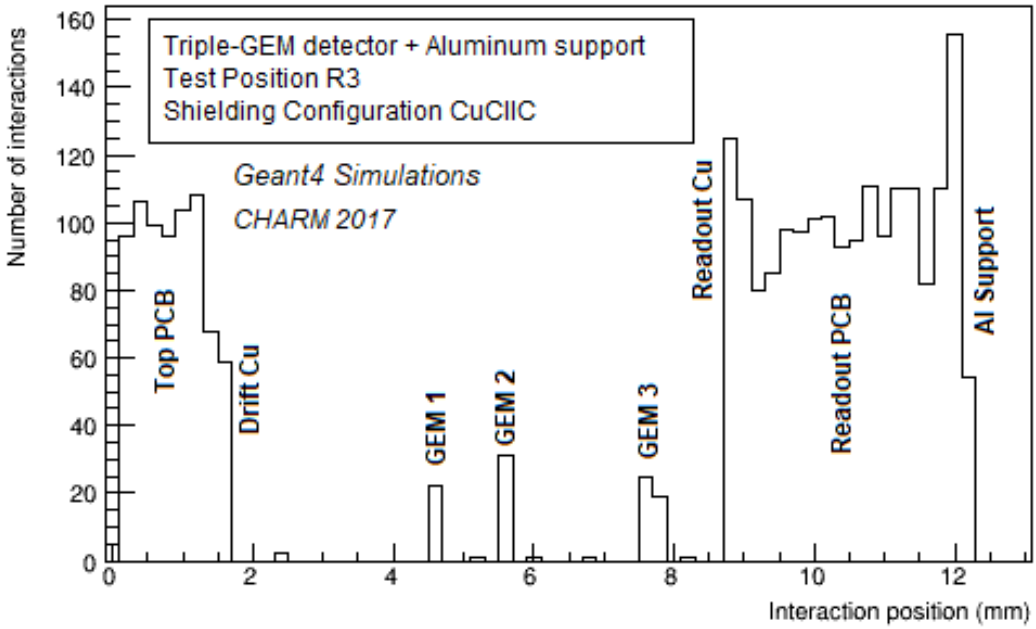

Figure 13. Position of the interactions undergone by neutrons in the Triple- GEM detector, when also the aluminum support is simulated.

6 Discharge probability measurement

6.1 Experimental setup

The readout system for the discharge probability studies, sketched in figure 14, consisted of four main parts:

- A CAEN A1515TG [7] multi-channel HV power supply was used to monitor the operating current and the high voltage in all the individual channels. The module was configured to operate in *GEM mode*, with a current limit on each channel set 1 μA above the average current measured with beam on and a trip time of 1 sec.
- A KEITHLEY 6487 [15] picoammeter was connected to the readout board to measure the anode current, which reflects the effective gas gain of the detector. The picoammeter was configured to sample the anode current with 40 sequential measurements at a rate of about 80 Hz, i.e. an anode current measurement every ~12.5 ms for a total sampling time of ~500 ms, to cover the whole PS spill length.
- A NIM+VME-based data acquisition system was employed to measure the interaction rate. The readout of the detector was done using a charge sensitive preamplifier connected to the bottom electrode of the third GEM-foil. The output of the preamplifier was sent to an

amplifier + shaper unit and then to a timing single channel analyzer unit. The timing single channel analyzer unit was operated in integral mode and the lower level in the unit was used as the threshold to the signal. The threshold was set at 0.5 V to reject the noise. The resulting digital pulses go through a NIM/ECL adapter to a scaler unit for the rate measurement.

- An enviromental Monitoring System based on ARDUINO Mega 2560 microcontroller [16] was designed to monitor the environmental parameters (atmospheric pressure, temperature) within the experimental irradiated area. Unfortunately, the ARDUINO board stopped working during the irradiation, probably due to radiation-induced damage even though it was installed in a cold zone. For this reason, all the data presented in the paper are not corrected for the environmental conditions.

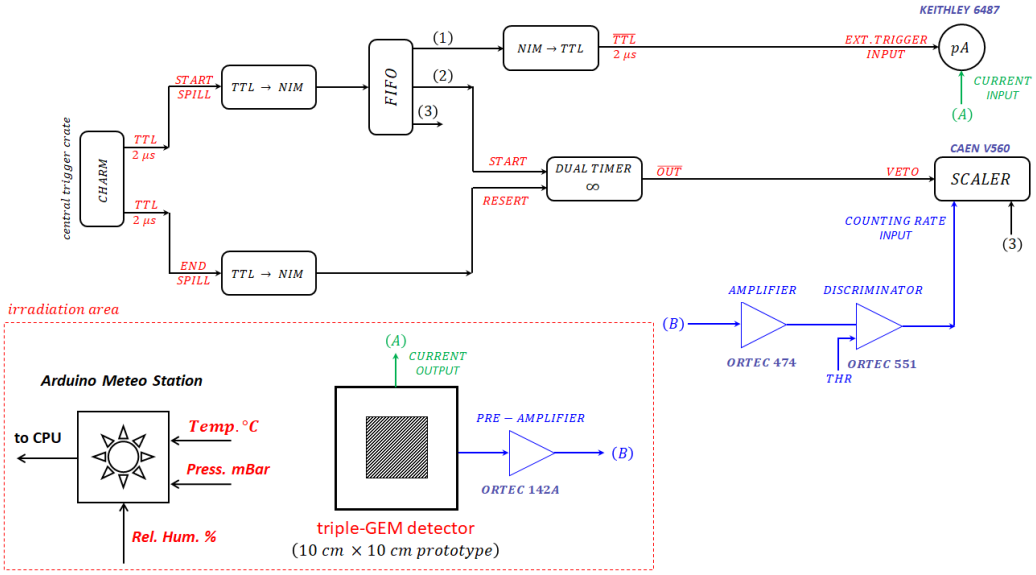

Figure 14. Sketch of the experimental setup used at CHARM.

The picoammeter was configured in external trigger mode to measure the anode current from the detector readout board in sync with the 24 GeV proton beam extracted from the PS accelerator and directed onto the copper target inside the CHARM experimental area.

6.2 Discharge identification methods

The discharge probability under neutron irradiation was measured combining the information coming from the anode current, readout from the readout pads using the picoammeter, and the operating current and voltage information provided by the CAEN A1515TG multi-channel HV power supply. If a discharge occurs in one of the three GEM-foils, the corresponding potential difference will drop. As a consequence, the gas gain for one of the three GEM-foils is temporarily reduced and a lower anode current is measured on the anode. Alternatively, the possible occurrence of a discharge in the Triple-GEM detector under test can be identified through a drop in the counting rate of the signals induced on the lower electrode of the third GEM-foil.

Another way of determining the occurrence of a discharge during a spill is to measure the operating current from the individual channels and to observe an increase in the current value,

2020 JINST 15 P10013

particularly from the upper electrode of the three GEM-foils. Thus, the occurrence of a discharge can alternatively be determined from such a sudden operating current increase on any one of the electrodes of the three GEM-foils, which eventually causes the HV channel to trip. An increase in the number of trips indicates then an increase in the number of discharges. This method has one particular advantage: it not only yields the number of discharge in a particular supply channel, but it may also point to the particular GEM-foil where the discharge occurred.

6.3 Results

The information on the charge produced inside the Triple-GEM detector during a single PS spill at CHARM was obtained from the current readout with the picoammeter. The typical spill structure at CHARM, shown in figure 15, is characterized by a peak in intensity and a total length of about 325 ms, the picoammeter data allows the determination of the maximum and average current associated to the spill.

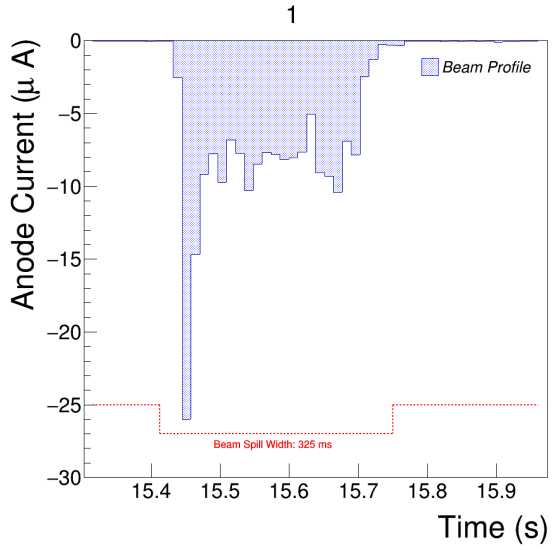

Figure 15. CHARM spill structure, as measured from the picoammeter.

The maximum current of each spill, figure 16 left, is obtained as

$$i_{\mathrm{MAX}} = \max_{\mathrm{j}} i_{\mathrm{j}} \tag{6.1}$$

where i_{j} are the 50 current measurements performed by the picoammeter in the single spill. The results, based on 23048 PS spills, show an average value of $21.5 \pm 5.2\,\mu\mathrm{A}$.

The average current of each spill, figure 16 right, is instead calculated as

$$i_{\mathrm{AV}} = \frac{\sum_{\mathrm{j=1}}^{50} i_{\mathrm{j}}}{50} \tag{6.2}$$

where i_j are the 50 current measurements performed by the picoammeter in the single spill. The results, based on 23048 PS spills, show an average value of $3.5 \pm 0.2\,\mu\mathrm{A}$.

2020 JINST 15 P10013

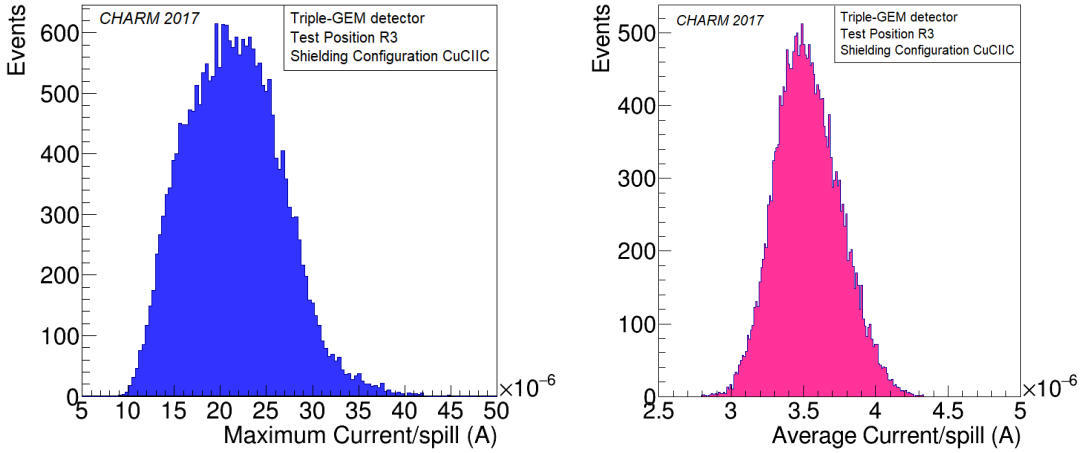

Figure 16. Maximum (left) and average (right) readout current within a spill for the Triple-GEM detector irradiated at CHARM.

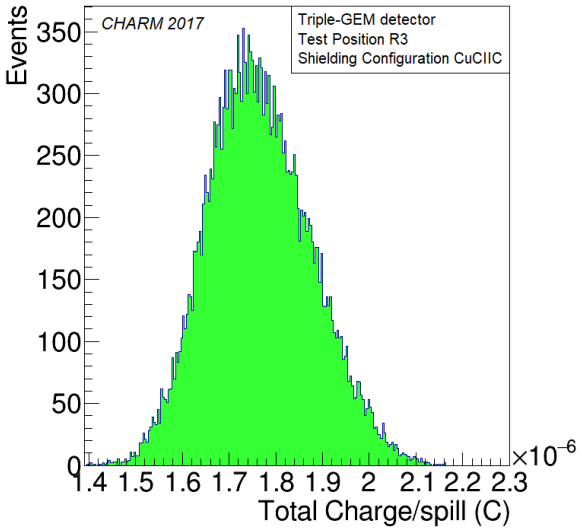

Figure 17. Total charge per spill for the Triple-GEM detector irradiated at CHARM.

The total charge per spill, figure 17, is then calculated as

$$q_{\mathrm{TOT}} = \sum_{\mathrm{j}=1}^{50} i_{\mathrm{j}} \times 10\,\mathrm{ms} \tag{6.3}$$

where i_j are the 50 current measurements performed by the picoammeter in the single spill and 10 ms is the average time used by the picoammeter for each single measurement. The results, based on 23048 PS spills, show an average value of 1.77 ± 0.11 μC/spill.

6.4 Dead time estimate

The dead time of the acquisition chain can be obtained from combination of the measured number of events detected by the NIM+VME system with the current measured by the picoammeter. Figure 18

2020 JINST 15 P10013

shows the measured number of events within a spill for the Triple-GEM detector irradiated at CHARM. The results, based on 23048 PS spills, show an average value $N^{\mathrm{MEA}} = (2.47 \pm 0.06) \times 10^5$ events per spill.

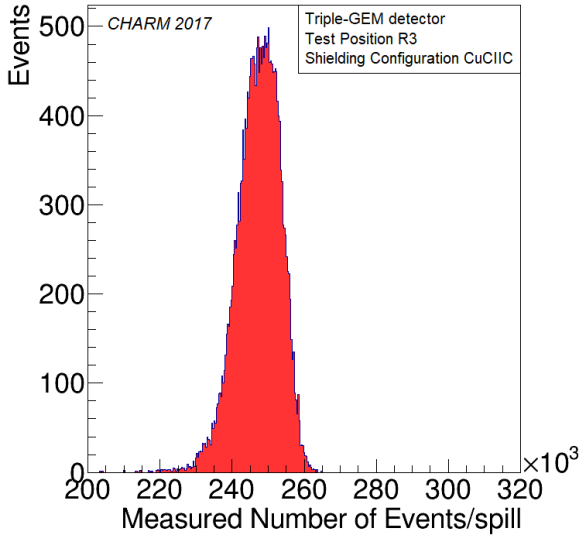

Figure 18. Measured number of events within a spill for the Triple-GEM detector irradiated at CHARM.

If instead we estimate the expected number of events within a spill from the current measured by the picoammeter, using the formula

$$N^{\mathrm{EST}} = \frac{i}{n_0 q_0 G} t_{\mathrm{SPILL}} \tag{6.4}$$

where i is the current in the spill, $n_0 = 100$, from Geant4 simulations, $q_0 = 1.6 \times 10^{-19}$ C, $G = 4 \times 10^4$, $t_{\mathrm{SPILL}} = 325$ ms is the length of the spill, the results are shown in figure 19.

The estimated number of events are $N^{\mathrm{EST}}_{\mathrm{MAX}} = (1.09 \pm 0.26) \times 10^7$ events per spill, using the maximum current in the spill, and $N^{\mathrm{EST}}_{\mathrm{AVE}} = (1.79 \pm 0.11) \times 10^6$ events per spill, using the average current in the spill, both much higher than the measured value.

An estimate of the dead time can be obtained from these results using the relation

$$N^{\mathrm{EST}} = \frac{N^{\mathrm{MEA}}}{1 - \frac{\tau N^{\mathrm{MEA}}}{t_{\mathrm{SPILL}}}} \tag{6.5}$$

from which

$$\tau = \frac{t_{\mathrm{SPILL}}}{N^{\mathrm{MEA}}} \left(1 - \frac{N^{\mathrm{MEA}}}{N^{\mathrm{EST}}}\right) \tag{6.6}$$

giving a dead time of 1.29 µs and 1.13 µs in the two cases.

2020 JINST 15 P10013

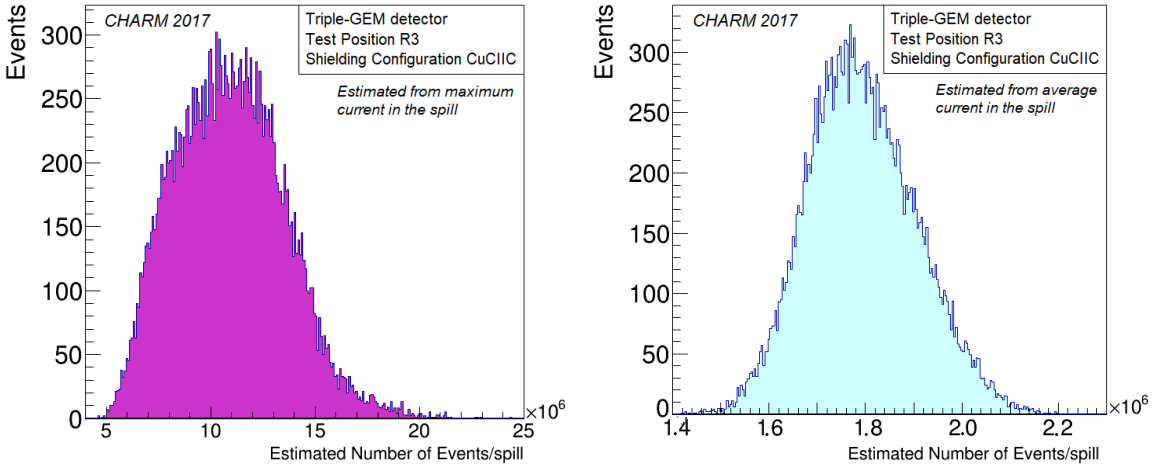

Figure 19. Estimated number of events within a spill for the Triple-GEM detector irradiated at CHARM using the maximum current in the spill (left) and the average current in the spill (right).

6.5 Discharge probability results

The estimate of the discharge probability/hit ($P_{\text{Discharge}}$) measured at CHARM with a Triple-GEM detector is shown in the box plot in figure 20. The values of discharge probability/hit used in this plot are obtained with the formula:

$$P_{\text{Discharge}} = \frac{N_{\text{Discharge}}}{N_{\text{COUNTS}} \times N_{\text{SPILL}}} \tag{6.7}$$

where N_{COUNTS} is the average number of counts, N_{SPILL} is the number of spills and $N_{\text{Discharge}}$ is the number of discharges detected in the test. Since this number was 0 at CHARM, we are using 3 as upper limit and, as a consequence, the $P_{\text{Discharge}}$ value is an upper limit as well. To set the upper limit the three-sigma rule [17, 18] is used for the discharge probability at 95% CL. In particular, four values have been calculated and included in the distribution of figure 20, corresponding to $N_{\text{COUNTS}} = N^{\text{EST}}_{\text{MAX}}$, $N_{\text{COUNTS}} = N^{\text{EST}}_{\text{AVE}}$, $N_{\text{COUNTS}} = N^{\text{MEA}}$ and $N_{\text{COUNTS}} = N^{\text{SIM}} = 5.84 \times 10^7$ events per spill. This last value is obtained from simulation as

$$N^{\text{SIM}} = \sum_{\text{k}} n_{\text{k}} \overline{S}_{\text{k}} f_{\text{k}} \tag{6.8}$$

where k is the index on the different particle species present in the CHARM radiation field, n_{k} is the number of particle per spill of a given species, $\overline{S}_{\text{k}}$ is the average sensitivity for a given species and f_{k} is the fraction of particles of a given species included in the radiation field. $\overline{S}_{\text{k}}$ for each particle species is obtained from figure 7 as

$$\overline{S}_{\text{k}} = \sum_{\text{E}} S_{\text{E}} f_{\text{E}} \tag{6.9}$$

where S_{E} is the sensitivity for a given particle species at a given energy and f_{E} is the fraction of particles of that energy composing the radiation field.

At the CHARM facility a value of $P_{\text{Discharge}} < 3.6 \times 10^{-11}$/hit at 95% CL is measured.

2020 JINST 15 P10013

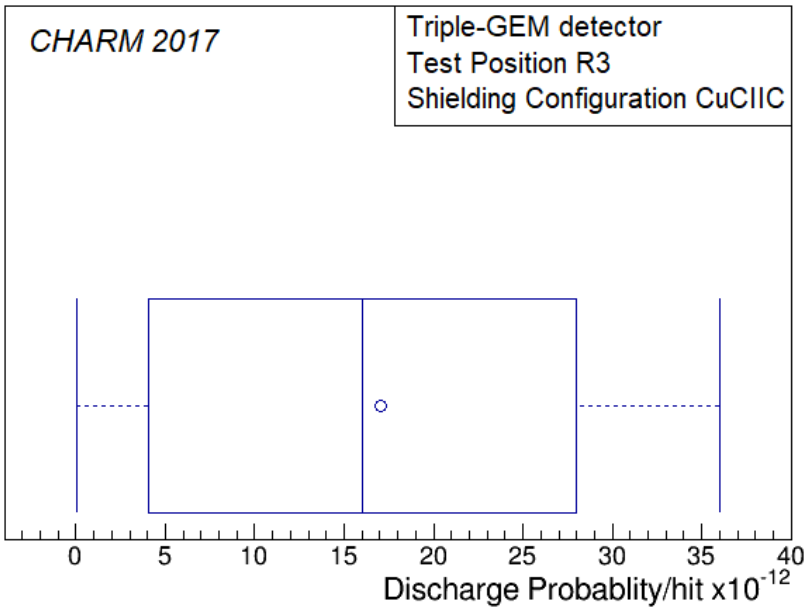

Figure 20. Estimation of the discharge probability per hit measured at CHARM with a Triple-GEM detector. The blue line in the middle of the box shows the median of the distribution, the box limits are the first and third quartile, while the error bars show the maximum and the minimum values of the distribution.

7 Comparison with previous results

A previous test was performed at CHARM in 2016 [2], with a measured upper limit of the discharge probability/neutron of 2.85×10^{-9}/hit at 95% CL. The new result (2017) lowers the limit previously set (2016) by almost two orders of magnitude. The improvement is justified considering the differences between the two tests: first of all, in 2017 the chamber was operated at a higher gain (4×10^4 vs. 3.5×10^4). In addition, the level of noise in the setup in 2017 was much lower than in 2016, which allowed us to set a threshold limit on the discriminator 5 times lower than in the past (100 mV vs. 500 mV). The corresponding measured event rate in 2016 was of the order of 1.75×10^5 events per spill [6], which is compatible with the average value measured in 2017 (2.47×10^5 events per spill). The estimated interaction rate evaluated from the current measurements is of the order of 10^7 events per spill without any correction for the dead time of the readout electronics. The results obtained in 2017 is also consistent with the results of measurement performed by other groups with similar detector geometries and slightly different gas mixtures, presented in detail in refs. [9, 10].

The expected number of discharges during detector operation in CMS based on the new CHARM results can be obtained from

$$N_{\text{Discharges}} = P_{\text{Discharge}} \times R_{\text{max}} \times t_{\text{LHC}} \tag{7.1}$$

where R_{max} is the maximum expected neutron fluence in the hottest region of the detector and t_{LHC} is the effective exposure time after ten HL-LHC years [6]. Table 1 shows the results obtained using 2016 and 2017 CHARM values. The calculation is performed using the total neutron fluence in the three regions; the neutrons with energy >1 MeV, which are more likely to produce a discharge in the detector, are ~20% of the total.

2020 JINST 15 P10013

Station	Expected number of discharges CHARM 2016 (1/cm^2)	Expected number of discharges CHARM 2017 (1/cm^2)
GE1/1	85	1
GE2/1	58.5	0.7
ME0	1124	14.2

Table 1. Expected number of discharges in GE1/1, GE2/1 and ME0 after ten years of operation at HL-LHC.

8 Conclusions

The discharge probability test for Triple-GEM detectors carried out in 2017 at the CERN CHARM irradiation facility has been presented. The results of the dedicated Geant4 simulation developed to analyze the behavior of the detector in a radiation environment, have been discussed as well. The result in terms of discharge probability/interacting particle sets an upper limit at 3.6×10^{-11}/hit, a difference of almost two orders of magnitude with respect to the limit previously set (2016), which could be justified considering the lower gain used in the second test and with the proper estimation of the incident particle rates.

Acknowledgments

We gratefully acknowledge the support from FRS-FNRS (Belgium), FWO-Flanders (Belgium), BSF-MES (Bulgaria), BMBF (Germany), DAE (India), DST (India), UGC (India), CSIR (India), INFN (Italy), NRF (Korea), QNRF (Qatar), and DOE (U.S.A.) and the RD51 collaboration.

References

[1] A. Colaleo, A. Safonov, A. Sharma and M. Tytgat, *CMS Technical Design Report for the Muon Endcap GEM Upgrade*, CERN-LHCC-2015-012 (2015) [CMS-TDR-013].

[2] CMS collaboration, *The Phase-2 Upgrade of the CMS Muon Detectors*, CERN-LHCC-2017-012 (2017) [CMS-TDR-016].

[3] F. Sauli, *GEM: A new concept for electron amplification in gas detectors*, *Nucl. Instrum. Meth. A* **386** (1997) 531.

[4] J. Merlin, *Study of long-term sustained operation of gaseous detectors for the high rate environment in CMS*, Thèse de doctorat, École doctorale Physique et Chimie-Physique, Strasbourg France (2016) and online at http://www.theses.fr/2016STRAE005.

[5] D. Pfeiffer et al., *The radiation field in the Gamma Irradiation Facility GIF++ at CERN*, *Nucl. Instrum. Meth. A* **866** (2017) 91 [arXiv:1611.00299].

[6] F. Fallavollita, *Triple-Gas Electron Multiplier technology for future upgrades of the CMS experiment: construction and certification of the CMS GE1/1 detectors and longevity studies*, Ph.D. Thesis, Università di Pavia, Pavia Italy (2019) [CERN-THESIS-2018-349] and online pdf version at https://cds.cern.ch/record/2658126/files/CERN-THESIS-2018-349.pdf.

[7] CAEN, *A1515*, (2020) https://www.caen.it/products/a1515/.

2020 JINST 15 P10013

[8] S. Bachmann et al., *Discharge mechanisms and their prevention in the gas electron multiplier (GEM)*, *Nucl. Instrum. Meth. A* **479** (2002) 294.

[9] G. Bencivenni et al., *Advances in triple-GEM detector operation for high-rate particle triggering*, *Nucl. Instrum. Meth. A* **513** (2003) 264.

[10] G. Bencivenni et al., *Performance of a triple-GEM detector for high rate charged particle triggering*, *Nucl. Instrum. Meth. A* **494** (2002) 156.

[11] G. Croci et al., *Discharge probability measurement of a Triple GEM detector irradiated with neutrons*, *Nucl. Instrum. Meth. A* **712** (2013) 108.

[12] A. Thornton, *CHARM Facility Test Area Radiation Field Description*, CERN-ACC-NOTE-2016-0041 (2016).

[13] A. Infantino, *FLUKA Monte Carlo Modelling of the CHARM Facility's Test Area: Update of the Radiation Field Assessment*, CERN-ACC-NOTE-2017-0059.

[14] GEANT4 collaboration, *GEANT4 — A simulation toolkit*, *Nucl. Instrum. Meth. A* **506** (2003) 250.

[15] Keithley Instruments, Inc., *Model 6487 Picoammeter/Voltage Source. User's Manual*, (2002) and online pdf version at https://usermanual.wiki/Document/Keithley6487Manual.2553076642/view.

[16] Arduino, *ARDUINO MEGA 2560 REV3*, (2020) https://store.arduino.cc/mega-2560-r3.

[17] L. Kazmier, *Business Statistics*, in *Schaum's Outline*, McGraw Hill Professional (2003).

[18] E.W. Grafarend, *Linear And Nonlinear Models: Fixed Effects, Random Effects, And Mixed Models*, Walter de Gruyter (2006).

2020 JINST 15 P10013